Effect of acid corrosion on the surface roughness and floatability of magnesite and dolomite

Xiufeng Gong[a,b,c], Jin Yao[a,b,c,*], Wanzhong Yin[c,**], Xueming Yin[c], Xiaoqi Ban[c], Yulian Wang[d,**]

[a] State Key Laboratory of Mineral Processing, Beijing 102628, China
[b] Key Laboratory of Solid Waste Treatment and Resource Utilization of the Ministry of Education, Southwest University of Science and Technology, Mianyang 621010, China
[c] School of Resources and Civil Engineering, Northeastern University, Shenyang 110819, China
[d] School of Materials Science and Engineering, Shenyang Ligong University, Shenyang 110159, China

ARTICLE INFO

Keywords:
Acid corrosion
Surface roughness
Flotation rate
Magnesite
Dolomite

ABSTRACT

To modify surface roughness and improve flotation performance, hydrochloric acid etching pretreatment was performed on magnesite and dolomite. Flotation tests disclosed that acid corrosion improved the flotation kinetics and flotation recovery rates of magnesite and dolomite. Under pulp pH 10 and sodium oleate (NaOl) concentration 20 mg·L^{-1}, the flotation recovery rates of magnesite and dolomite after acid etching increased by 31.05% and 29.20%, respectively, compared with those before acid etching. Adsorption density tests proved that the adsorption density of NaOl on magnesite and dolomite was higher after acid etching than before acid etching, implying that acid etching drives NaOl adsorption. Zeta potential analysis revealed that acid etching reduces the point of zero charge of magnesite and dolomite. Atomic force microscopy and X-ray photoelectron spectroscopy results demonstrated that acid corrosion modified the surface roughness of magnesite and dolomite, increasing the magnesium (Mg) content on the magnesite surface and the calcium and Mg contents on the dolomite surface. Contact angle measurements indicated that acid corrosion slightly reduced the contact angle between magnesite and dolomite. With NaOl present on the surface, the contact angles of magnesite and dolomite after acid etching significantly increased compared with those before acid etching. Therefore, acid etching is effective in improving the floatability of magnesite and dolomite.

1. Introduction

Magnesium (Mg) is the eighth most common element in earth's crust and the third most common metal after aluminum and iron [1]. Currently, Mg, Mg alloys, and Mg-based composite materials are extensively employed in refractory materials and the automobile, medical, military, and aerospace industries [2,3]. China has abundant Mg reserves, and magnesite, brucite, dolomite, and serpentine are common Mg-containing minerals [4,5]. Magnesite is a high-quality mineral; however, its mining leads to resource waste [6]. The intense economic growth in China has brought about the high-value utilization of low-grade magnesite [7]. The key to the efficient utilization of magnesite is to reduce the dolomite content, which is the main gangue mineral of magnesite [8,9].

Flotation, an effective method for mineral enrichment, fully uses the surface characteristics of minerals and is widely used in industrial production [10]. Flotation is influenced by mineral, chemical, and particle size composition, reagent systems, working characteristics of the flotation machine, and operational factors [11]. Among these, the physical and chemical properties of the raw materials significantly influence the flotation process [12,13]. Therefore, the effects of changes in these properties on the floatability of minerals warrant an investigation.

The surface properties of minerals have been extensively studied in flotation research. Selective modifications of the surface characteristics of minerals by surface pretreatment methods can improve their floatability, such as morphology, charge properties, and adsorption characteristics [14–16]. Acid etching is an effective chemical treatment

method that changes the surface properties of minerals via chemical or electrochemical interactions with acidic media [17–19]. Assessment of the microscopic differences in these surface properties must be performed to shed light on the effects of acid etching.

Acid etching changes the surface properties of minerals, thus affecting the adsorption performance of flotation reagents and the flotation recovery rate of minerals. Zhu *et al.* [20] found that oxalic acid pretreatment enhanced and reduced the adsorption capacity of sodium oleate (NaOl) on bauxite and kaolinite. Zhang *et al.* [21] observed that sulfuric acid etching decreased the Al/Si atomic ratio on the surface of kaolinite compared with natural kaolinite, decreasing the adsorption performance of the inhibitor sodium hexametaphosphate and improving the adsorption ability of the collector dodecylamine hydrochloride. Parapari *et al.* [22] demonstrated that acid etching is a reliable and preferred pretreatment method to modify the surface characteristics of ilmenite and improve its floatability, as well as reduce the floatability of the gangue minerals olivine and pyroxene and improve the separation selectivity and efficiency of mineral flotation without inhibitors [23]. Feng *et al.* [24] could not achieve the flotation separation of talc and serpentine with an inhibitor, i.e., sodium carboxymethyl cellulose, before acid etching. After acid etching, the point of zero charge of serpentine decreased from 10.2 to 6.8, and the negatively charged serpentine did not interfere with the inhibitory effect of sodium carboxymethyl cellulose on talc.

Reports on the hydrochloric acid etching of magnesite and dolomite as a pretreatment step are scant; magnesite and dolomite belong to the same category of alkaline earth carbonate minerals. In this work, magnesite and dolomite were pretreated with hydrochloric acid, followed by single-mineral flotation experiments and flotation kinetics studies. The effects of acid etching on the surface properties of both minerals were examined in depth by evaluation of the changes in surface adsorption performance, surface charge, surface element content, surface roughness, and surface wettability before and after acid etching. This study provides new insights into the flotation of magnesite resources.

2. Materials and methods

2.1. Materials

High-grade magnesite and dolomite bulk ores were obtained from Dashiqiao Mining Area, Yingkou City, Liaoning Province, and Quyang Mining Area, Baoding City, Hebei Province, respectively. Pure minerals were extracted by manually crushing the ores, hand picking, removal of impurities, mortar grinding, and screening. Mineral particles with particle sizes of − 0.074 + 0.038 mm were taken as samples for flotation tests [25].

In Fig. 1, the XRD patterns of magnesite and dolomite are consistent with their standard PDF cards (PDF#08–0479 and PDF#36–0426, respectively) [26]. In Table 1, the multielement analysis results indicate that magnesite contains 47.12wt% MgO, with 98.56% purity. The MgO and CaO contents in dolomite are 20.95wt% and 29.92wt%, respectively, with 98.42% purity. Both minerals are of very high purity, which satisfies the requirements of single-mineral experiments.

Table 1
Multielement analysis (wt%).

Sample	MgO	CaO	SiO_2	Al_2O_3	TFe	Purity
Magnesite	47.12	0.65	0.75	0.15	0.15	98.56
Dolomite	20.95	29.92	—	—	—	98.42

2.2. Etching test

Etching using hydrochloric acid as the etchant was performed. A flotation-grade single mineral (magnesite or dolomite) and hydrochloric acid (0.025–0.125 mol·L^{-1}) were placed in a beaker in a 1:4 ratio (solid-to-liquid, by mass) under stirring at 1200 r/min for even mineral dispersion in the etching solution. The solution was then cleaned repeatedly with deionized water, followed by filtration and low-temperature drying, finally furnishing the sample for flotation tests.

2.3. Flotation test

The flotation test was performed using an XFG II flotation machine at a fixed speed of 1992 r/min.

(1) For the single-mineral flotation experiment, 20 mL of deionized water was added to a flotation tank with 2.0 g of ore sample and mixed for 2 min. The pH of the slurry was then adjusted to 3. NaOl was added to the slurry and stirred for 3 min, followed by froth scraping for 4 min. The concentrate and tailings were dried and weighed separately, and the recovery rate was calculated [27].
(2) For the flotation dynamics test, the same steps for the single-mineral flotation test were conducted, but foam products were scraped based on the time intervals of flotation dynamics (0–0.2, 0.2–0.4, 0.4–0.6, 0.6–1, 1–2, 2–4, 4–6, and 6–8 min). The fitting equations for the flotation dynamics model are listed in Table 2.

In these formulas, t is the cumulative flotation time, R is the cumulative recovery rate after time t, R_∞ is the theoretical maximum recovery rate, and k is the flotation rate constant (min^{-1}).

2.4. Adsorption density measurements

The adsorption density of NaOl on the surfaces of magnesite and dolomite before and after acid etching was measured using a

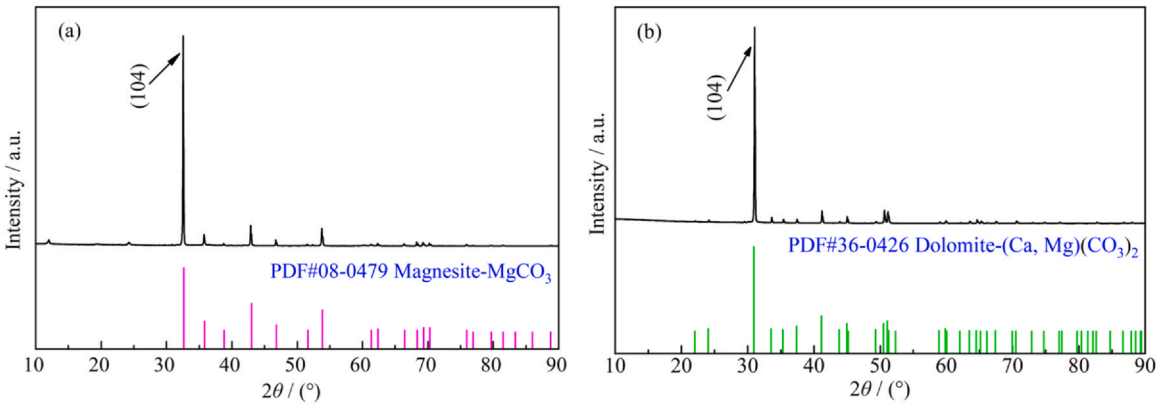

Fig. 1. XRD patterns of (a) magnesite and (b) dolomite.

Table 2
Flotation kinetics models.

Serial number	Flotation kinetic models	Equation
1	Classical first-order kinetic model [28] (M1)	$R = R_\infty[1 - \exp(-k_1 t)]$
2	First-order matrix distribution model [29] (M2)	$R = R_\infty\left\{1 - \frac{1}{k_2 t}[1 - \exp(-k_2 t)]\right\}$
3	Second-order dynamic model [30] (M3)	$R = R_\infty^2 k_3 t/(1 + R_\infty k_3 t)$
4	Second-order matrix distribution model [31] (M4)	$R = R_\infty\left\{1 - \frac{1}{k_4 t}[\ln(1 + k_4 t)]\right\}$

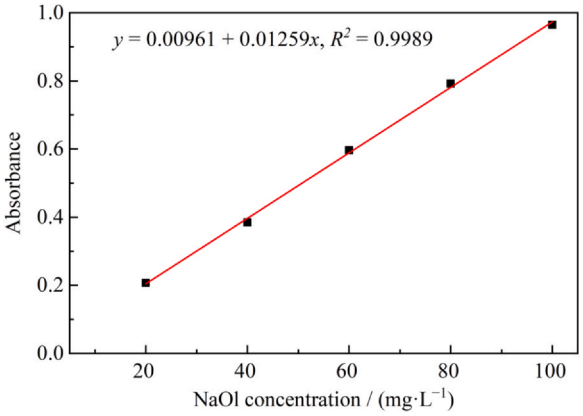

Fig. 2. NaOl adsorption isotherm.

UV1901PC UV spectrophotometer. The characteristic absorption peak of NaOl was observed at 231 nm [32]. The adsorption isotherm curve was constructed by measuring the absorbance of NaOl at concentrations of 20, 40, 60, 80, and 100 mg·L^{-1}, and the curve is plotted in Fig. 2.

The residual concentration of NaOl in the solution after interaction with minerals was obtained using the adsorption isotherm (Fig. 2). The adsorption density of NaOl on the mineral surface can be calculated using

$$\Gamma = \frac{(c_0 - c_1)V}{m} \quad (1)$$

where Γ is the adsorption density of NaOl (mg·g^{-1}), c_0 and c_1 are the initial and residual concentrations (mg·L^{-1}) of the NaOl solution, respectively, V is the volume of the NaOl solution (neglecting the volume changes before and after adsorption, L), and m is the mass (g) of the magnesite or dolomite sample.

2.5. Dynamic potential measurement

The dynamic potentials of the minerals were determined using a Nano-ZS90 Marvin dynamic potential analyzer (Britain). The minerals were finely ground in an agate mortar to ~5 μm. Single-mineral particles were weighed to 20 mg with an analytical balance and placed in 40 mL of 1×10^{-3} mol·L^{-1} potassium chloride solution. The pH was adjusted with HCl and NaOH. The solution was stirred for 5 min using a magnetic stirrer and maintained for another 10 min [33]. Afterward, the test was conducted with the supernatant. The average of six measurements was taken as the final dynamic potential for each sample.

2.6. X-ray photoelectron spectroscopy

Surface elemental composition was determined using an X-ray photoelectron spectrometer (XPS, ESCALAB 250Xi). Under the optimal conditions of the acid-corrosion test, acid etching pretreatment was applied to the sample with ~5 μm particle size. The samples were passed through an Al K_α X-ray (photoelectron energy of 1486.6 eV) excitation source before and after acid etching to detect the photoelectron energy of the valence electrons of atoms or molecules on the test sample surface [34]. The test results were analyzed with Avantage software and calibrated with C 1s charge (284.8 eV).

2.7. Surface topography analysis

The surface morphology characteristics of magnesite and dolomite before and after acid etching were determined using a MultiMode 8 atomic force microscope [35], and the results were analyzed with NanoScope Analysis software.

2.8. Contact angle measurement

Contact angle measurements were performed using a JC2000 contact angle tester [36]. After reaction with the flotation reagents, the samples were filtered and air-dried. The dried sample was then pressed using a tablet press in smooth and dense thin sheets and placed on a measuring table. Deionized water was dropped with a microsyringe onto the surface of the ore sample to measure the contact angle. A high-speed camera (CCD) was used to record the contact angle of the droplets on the surface of the ore sample. The average of three measurements was taken as the final contact angle of each sample.

3. Results and discussion

3.1. Analysis of the flotation results

3.1.1. Acid etching time

The plot of acid etching time–recovery rate for magnesite and dolomite at 60 mg·L^{-1} NaOl and 0.100 mol·L^{-1} etching solution is shown in Fig. 3.

Fig. 3 indicates that with increasing acid etching time, the flotation recovery rates of magnesite and dolomite first quickly increased and then plateaued. For the magnesite sample, its flotation recovery rate before acid etching was 82.20%, which increased to 92.60% and 98.15% when increasing the acid etching time to 5 and 15 min, respectively, reaching its maximum value at 15 min. For the dolomite sample, the flotation recovery rate before acid etching was 87.30% and

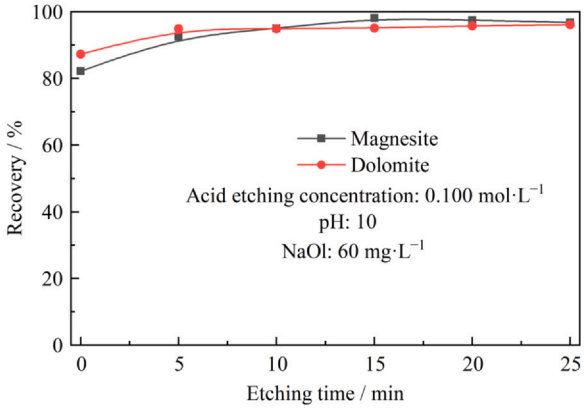

Fig. 3. Effect of acid etching time on the floatability of magnesite and dolomite.

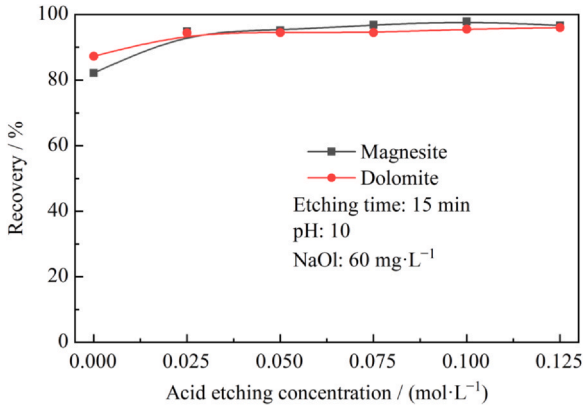

Fig. 4. Effect of the etching solution concentration on the floatability of magnesite and dolomite.

increased to 94.90% and 96.14% when the acid etching time increased to 5 and 15 min, respectively. Magnesite achieved a maximum recovery rate at 15 min; thus, the effect of the etching solution concentration on the recovery rates of magnesite and dolomite was studied for an acid etching time of 15 min.

3.1.2. Etching solution concentration

The effect of the etching solution concentration on the recovery rates of magnesite and dolomite for an acid etching time of 15 min is plotted in Fig. 4.

In Fig. 4, the flotation recovery rates of magnesite and dolomite increased after acid etching. In 0.025 mol·L^{-1} etching solution, the flotation recovery rate of magnesite increased from 82.20% to 94.85%, and that of dolomite increased from 87.30% to 94.40%, showing improvement in floatability of both minerals by acid etching. Because magnesite achieved a maximum flotation recovery rate of 97.95% in 0.100 mol·L^{-1} etching solution and the difference in flotation recovery rates between the two minerals was the largest, the optimal conditions for acid etching were an etching solution concentration of 0.100 mol·L^{-1} and an acid etching time of 15 min.

3.1.3. NaOl concentration

The effect of NaOl concentration on the floatability of magnesite and dolomite before and after acid etching in pH 10 fixed slurry is plotted in Fig. 5.

Fig. 5 shows that with increasing NaOl concentration, the flotation recoveries of magnesite and dolomite after acid etching increased to a certain extent compared with those before acid etching, and gradually stabilized. Thus, acid etching increased the flotation recovery rates of magnesite and dolomite and promoted the adsorption of NaOl for both minerals.

3.1.4. Pulp pH

The effect of pulp pH on the floatability of magnesite and dolomite before and after acid etching with 60 mg·L^{-1} NaOl is plotted in Fig. 6.

Fig. 6 shows that with an increase in pulp pH, the flotation recovery rates of magnesite and dolomite before and after acid etching first increased and then decreased. The flotation recovery rates of both minerals after acid etching were higher than those before acid etching. Thus, acid etching improved the flotation recovery rates of magnesite and dolomite.

3.1.5. Flotation kinetics

The nonlinear fitting of flotation kinetics can reveal the differences in flotation characteristics between magnesite and dolomite before and after acid etching. Fig. 7 shows the nonlinear fitting of the cumulative recovery rates of magnesite and dolomite under 60 mg·L^{-1} NaOl and pulp pH 10.

From Fig. 7, the time it took magnesite and dolomite to reach the maximum flotation recovery rate after acid etching was shorter than before acid etching, demonstrating that acid etching improves the flotation kinetics of both minerals. Their maximum flotation recovery rates were higher after acid etching than before acid etching, indicating that acid etching improves NaOl adsorption for both minerals. At 8 min, the cumulative recovery rates of magnesite flotation before and after acid etching reached 93.00% and 97.30%, respectively, whereas those of dolomite flotation reached 93.85% and 98.85%, respectively. Comparison of the cumulative flotation recovery rates of the two minerals before and after acid etching verified that acid etching considerably improves the flotation recovery rates of magnesite and dolomite.

Flotation kinetic parameters, i.e., fitting correlation rate (R^2), theoretical recovery rate (R_∞), and flotation rate constant (k value), are crucial for the flotation process. Table S1 summarizes the flotation kinetic parameters of magnesite and dolomite. The classical first-order kinetic model (M1) and first-order matrix distribution model (M2) were a good fit for the cumulative recovery rate of magnesite ($R^2 > 98\%$). Compared with M2, M1 had a better fit ($R^2 > 99\%$). The fitting performances of the second-order dynamics model (M3) and the second-order matrix distribution model (M4) were not as good as those of M1 and M2. For dolomite, M1 and M2 had a better fit after acid etching ($R^2 > 99\%$) than before acid etching ($R^2 > 98\%$).

In the M1 fitting, R_∞ and k were higher for magnesite and dolomite after acid etching than those before acid etching, indicating that magnesite has better flotation characteristics after acid etching. Similarly, their flotation recovery rates and flotation kinetics increased after acid etching. Table S1 reveals that the theoretical maximum recovery rate of M1 was near the experimental value, and M1 had the best fit. Moreover, magnesite possesses good flotation characteristics after acid etching. The fitting parameters of each particle size showed higher values after acid etching than before acid etching: the k values of magnesite and dolomite were higher after acid etching. The M1 of magnesite before

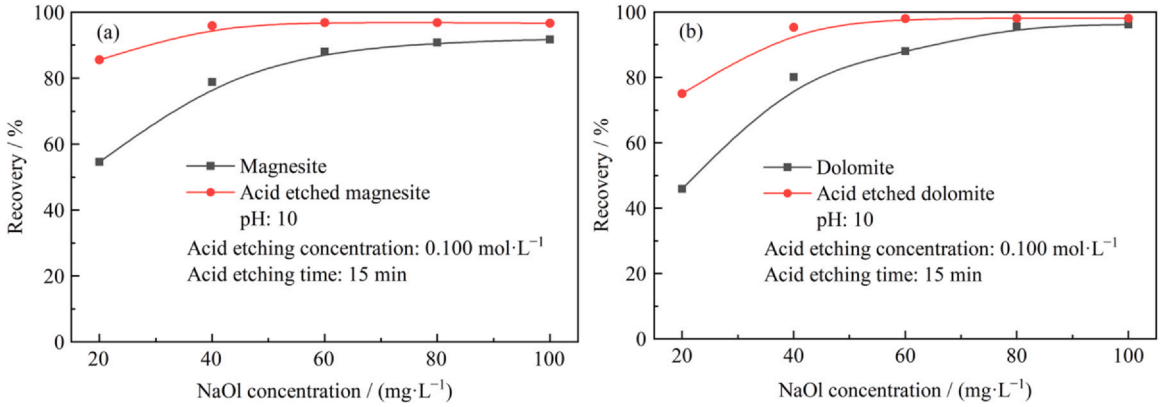

Fig. 5. Effect of NaOl concentration on the floatability of (a) magnesite and (b) dolomite before and after acid etching.

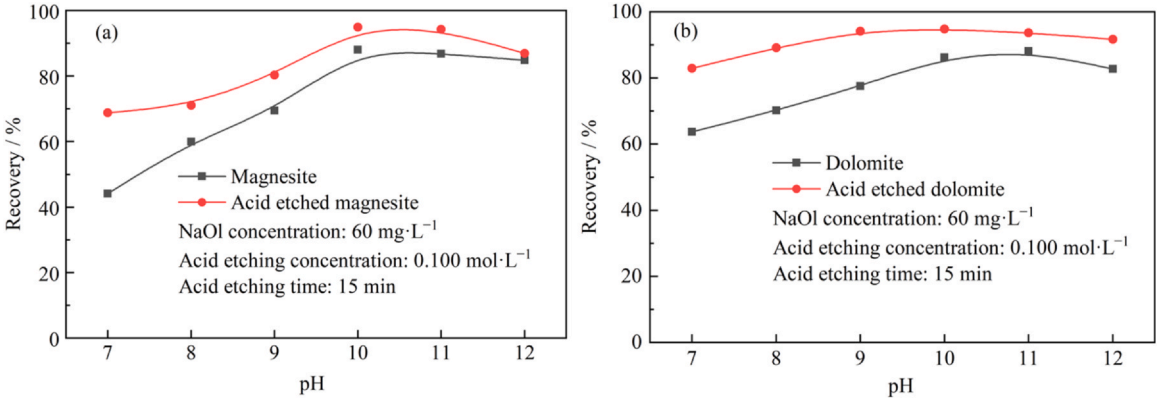

Fig. 6. Effect of pulp pH on the floatability of (a) magnesite and (b) dolomite before and after acid etching.

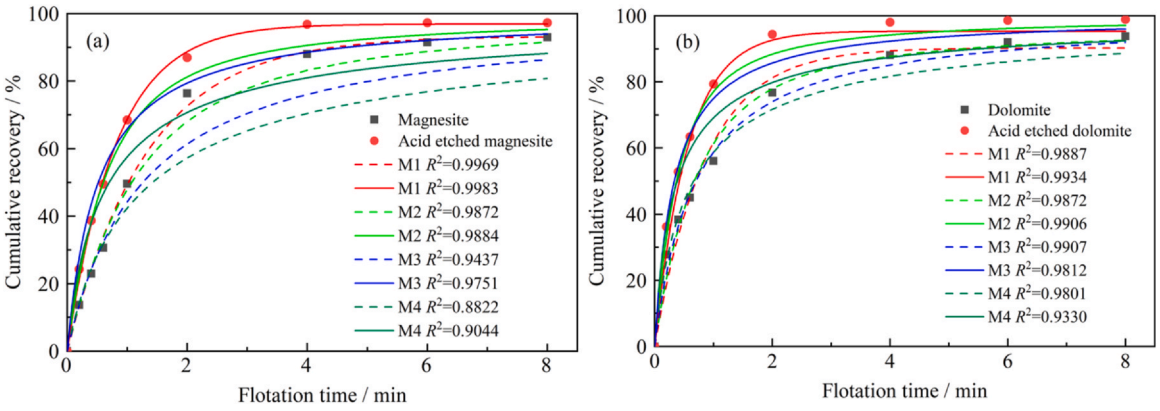

Fig. 7. Nonlinear fitting of flotation kinetics for cumulative recovery of (a) magnesite and (b) dolomite.

and after acid etching had k values of 0.7530 and 1.2363 min^{-1}, respectively, and that of dolomite showed k values of 1.1521 and 1.8781 min^{-1}, respectively.

3.2. Adsorption density analysis

The difference in the floatability of magnesite and dolomite can be studied based on the adsorption density of NaOl on their surfaces before and after acid etching. The results are illustrated in Fig. 8.

Fig. 8 shows that with increasing NaOl concentration, its adsorption density on the magnesite and dolomite surfaces before and after acid etching gradually increased; the adsorption density was higher after acid etching than before acid etching for both minerals. At 60 mg·L^{-1} NaOl, the NaOl adsorption densities on magnesite before and after acid etching were 0.44 and 0.49 mg·g^{-1}, and those on dolomite increased from 0.41 to 0.46 mg·g^{-1}, respectively; thus, the adsorption density increased by 0.05 mg·g^{-1} for both minerals after acid etching. These results show that acid etching improves the adsorption density of NaOl on magnesite and dolomite, which is suitable for the adsorption of the NaOl collector on the mineral surfaces.

3.3. Zeta-potential results

Fig. 9 exhibits that the zeta potentials of magnesite and dolomite decreased after acid etching and showed a certain degree of positive shift. The point of zero charge of magnesite decreased from 8.83 before acid etching to 8.61 after etching, whereas that of dolomite decreased from 6.90 before acid etching to 6.41 after etching. Therefore, acid etching decreased the point of zero charge of magnesite and dolomite, which is beneficial for NaOl adsorption on surfaces.

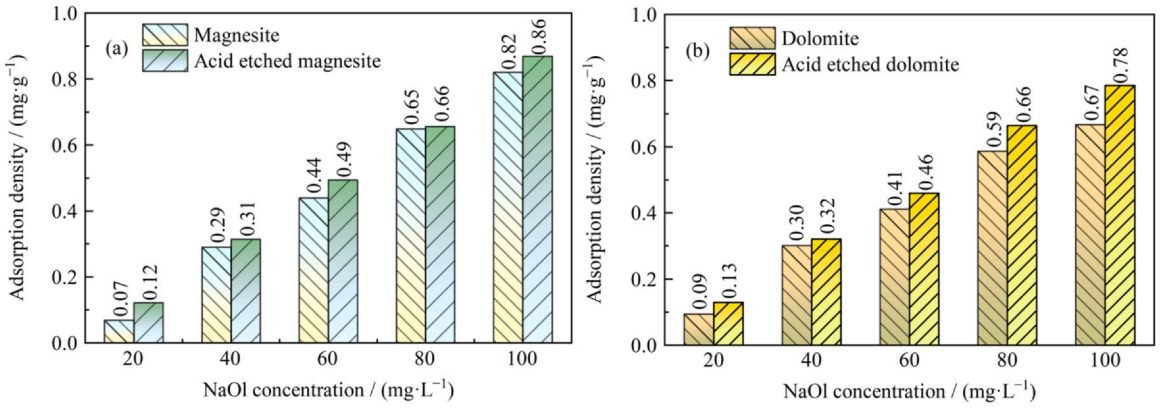

Fig. 8. Adsorption densities of NaOl on the (a) magnesite and (b) dolomite surfaces.

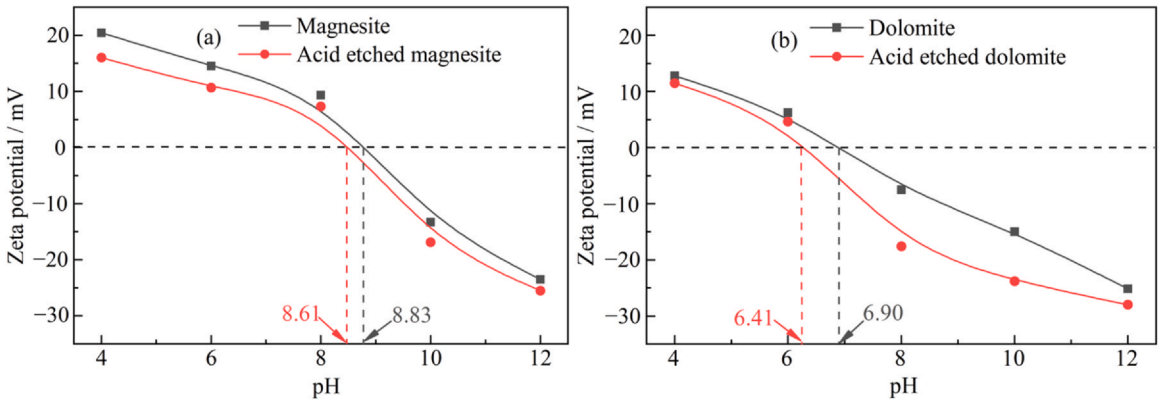

Fig. 9. Effect of pulp pH on the zeta potentials of (a) magnesite and (b) dolomite before and after acid etching.

3.4. XPS analysis

The surface element compositions of magnesite and dolomite before and after acid etching are summarized in Table 3.

Table 3 shows that the relative content of Mg on the surface of magnesite increased from 7.97at% to 8.55at% after acid etching, whereas those of Mg and Ca on the surface of dolomite increased from 1.97at% to 4.52at% and from 6.71at% to 9.60at%, respectively, demonstrating that after acid etching, additional Mg sites are exposed on the magnesite surface, whereas more Ca and Mg sites are exposed on the dolomite surface. In addition, the surface properties of magnesite and dolomite improved after acid etching, and the increase in Ca and Mg sites might be the reason for the improved flotation performance of the two minerals after acid etching.

3.5. Surface roughness analysis

Fig. 10 plots the surface roughness characteristics of magnesite and dolomite before and after acid etching. Here, R_a represents arithmetic roughness, and R_q represents root mean square roughness. Before acid etching, the rough body size of the magnesite was 0–0.60 nm, with R_a of 0.12 nm and R_q of 0.16 nm. After acid etching, the surface roughness of the magnesite was 0.50–2.40 nm, with R_a of 0.29 nm and R_q of 0.44 nm. Before acid etching, the surface roughness of the dolomite was 0.20–1.30 nm, with R_a of 0.16 nm and R_q of 0.26 nm. After acid etching, the surface roughness of the magnesite was 0.50–2.20 nm, with R_a of 0.21 nm and R_q of 0.37 nm. After acid etching, the roughness and roughness factors of magnesite and dolomite increased, which demonstrates that acid etching modifies the roughness of magnesite and dolomite and exposes more adsorption sites on their surfaces.

3.6. Surface wettability analysis

In Fig. 11, the contact angles of magnesite and dolomite before acid etching were 32.70° and 24.07°, respectively, but after acid etching, they decreased to 32.18° and 22.71°, respectively. With NaOl on the surfaces of minerals before acid etching, the contact angles of magnesite and dolomite were 58.63° and 64.82°, respectively, but after acid etching, they were 72.67° and 88.35°, respectively. These results indicate that the surface wettability of the two minerals was similar before and after acid etching. After acid etching, the contact angles for magnesite and dolomite slightly decreased, and their hydrophilicity slightly improved. With the presence of NaOl on the surfaces, the contact angles for magnesite and dolomite before and after acid etching considerably increased, and their hydrophobicity considerably improved. The contact angles of magnesite and dolomite increased by 14.04° and 23.53°, respectively, after acid etching compared with before acid etching. Thus, the adsorption energy of NaOl on the surfaces of the two minerals was stronger after acid etching.

Table 3
XPS analysis results of the relative contents of the elements on the magnesite and dolomite surfaces before and after acid etching.

Samples	Element / at%			
	C 1s	O 1s	Mg 1s	Ca 2p
Magnesite	39.50	52.53	7.97	—
Acid-etched magnesite	38.50	52.95	8.55	—
Dolomite	36.61	54.71	1.97	6.71
Acid-etched magnesite	38.24	47.94	4.52	9.60

3.7. Acid-corrosion mechanism

The flotation test disclosed the increased flotation recovery rates of magnesite and dolomite after acid etching. Combined with the flotation kinetics test, acid etching increased the flotation recovery rates of the two minerals and improved the collection ability of NaOl. Adsorption density measurements verified the stronger adsorption ability of NaOl on the mineral surfaces after acid etching. XPS demonstrated that acid etching can increase the Mg or Ca content in both minerals, exposing additional sites. Atomic force microscopy intuitively reflected the changes in surface roughness of the two mineral surfaces after acid etching. Based on the changes in contact angles, it can be inferred that the exposed Ca and Mg sites after acid etching were suitable for NaOl adsorption, which enhanced their hydrophobicity, facilitating their upward flotation. Based on the above results, it can be concluded that acid etching achieves an increase in surface roughness of the minerals, an increase in surface active sites, and an improvement in floatability. Acid etching can increase the surface roughness and active sites of minerals and expose the unexposed sites on the mineral surface, providing more adsorption sites for collectors and improving the floatability of magnesite and dolomite [12,37–39]. Fig. 12 depicts the possible acid-corrosion mechanism, indicating corrosion on the mineral surface sites and the floatability of magnesite and dolomite.

3.8. Shortcomings and prospects

In this study, flotation experiments and detection analysis are applied to study the effects of acid corrosion on the surface roughness, active sites, and floatability characteristics of magnesite and dolomite, and a good explanation of the relationship between the three is provided. However, the flotation separation of magnesite and dolomite is still a significant scientific problem, and this study lays a theoretical basis for the flotation separation of magnesite and dolomite. Based on the obtained results, after acid etching, flotation separation of the two minerals cannot be achieved only in the system of NaOl as the collector. Therefore, future research should investigate the synergistic effect of acid corrosion and regulators on the floatability and flotation separation of magnesite and dolomite, including systematic experimental

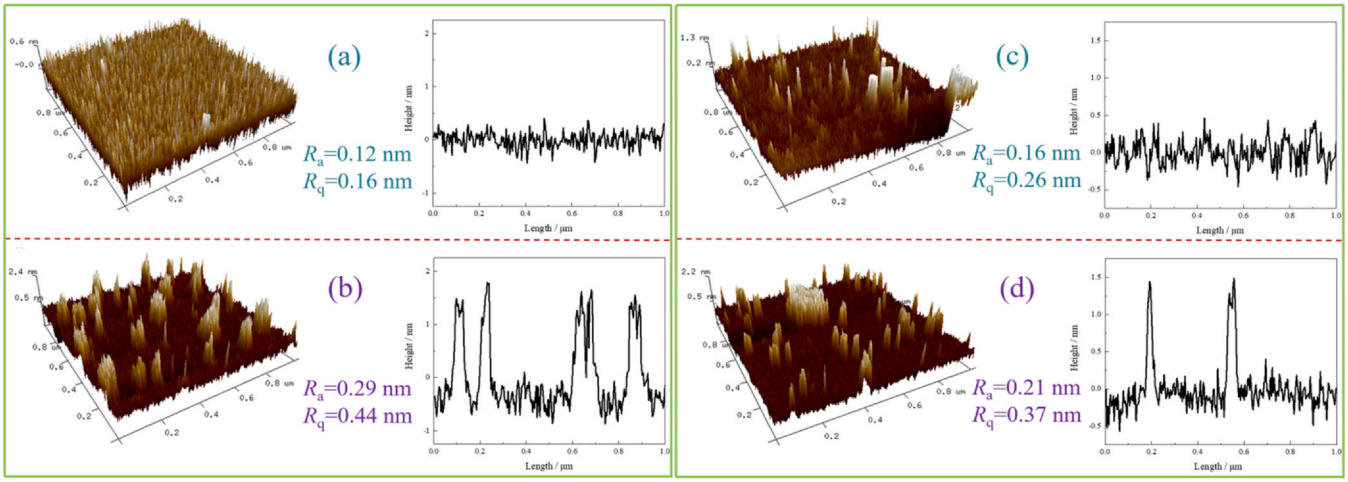

Fig. 10. Two-dimensional graph and cross-sectional height curve for (a) magnesite, (b) acid-etched magnesite, (c) dolomite, and (d) acid-etched dolomite surfaces.

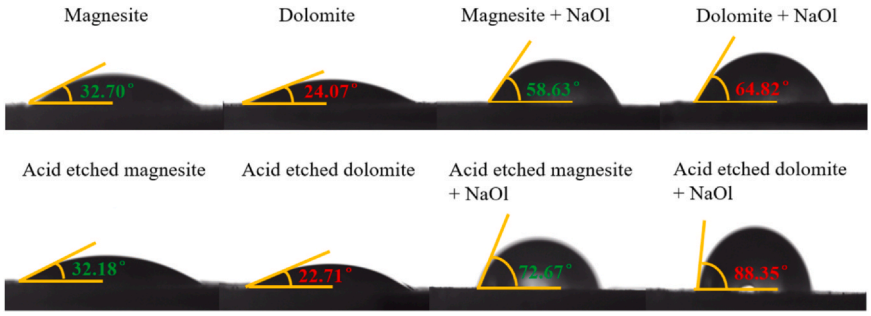

Fig. 11. Contact angles for magnesite and dolomite before and after acid etching.

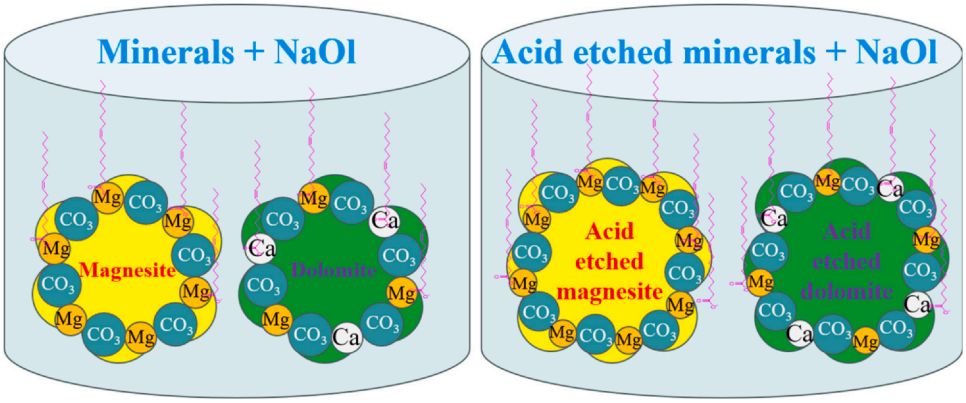

Fig. 12. Roles of acid corrosion on surface sites and floatability of magnesite and dolomite.

research on the choice of regulators. Moreover, considering the characteristic of acid corrosion simultaneously improving the flotation recovery of magnesite and dolomite, the inhibitory effect of regulators on magnesite and dolomite should be the focus of future research.

4. Conclusions

(1) After acid etching, the flotation recovery rates of magnesite and dolomite increased, with the highest increases of 31.05% and 29.20%, respectively, and the flotation kinetics became faster.
(2) Acid etching decreased the point of zero charge of magnesite and dolomite and increased the adsorption density, which is conducive to NaOl adsorption.
(3) Acid corrosion modified the morphological characteristics of magnesite and dolomite, exposing more Mg or Ca and Mg sites on the surfaces of magnesite and dolomite, respectively, and promoting NaOl adsorption.
(4) With NaOl, the contact angles of the magnesite and dolomite after acid etching were considerably higher than those before acid etching. Thus, acid etching is an effective method for improving the floatability of the two minerals.

CRediT authorship contribution statement

Xiufeng Gong: Methodology, Validation, Investigation, Writing - original draft, Writing – review & editing. **Jin Yao:** Supervision, Project administration. **Wanzhong Yin:** Conceptualization, Project administration. **Xueming Yin:** Writing – review & editing. **Xiaoqi Ban, Yulian Wang:** Visualization.

Declaration of Competing Interest

Wanzhong Yin is an editorial board member for this journal and was not involved in the editorial review or the decision to publish this article. The authors declare that they have no known financial interests or personal relationships that could have appeared to influence the work reported in this paper.

Acknowledgements

This work was financially supported by the Open Foundation of State Key Laboratory of Mineral Processing (No. BGRIMM-KJSKL-2024-07), the Open Project of the Key Laboratory of Solid Waste Treatment and Resource Utilization of the Ministry of Education, China (No. 23kfgk02), and the National Natural Science Foundation of China (Nos. 51974064, 52174239, and 52374259).

Appendix A. Supporting information

Supplementary data associated with this article can be found in the online version at doi:10.1016/j.gsme.2024.02.001.

References

[1] S. Rahimpour Golroudbary, I. Makarava, A. Kraslawski, Environmental assessment of global magnesium production, Miner. Process. Extr. Metall. Rev. 44 (6) (2023) 389–406.
[2] C.L. Adam, R.G. Hemingway, N.S. Ritchie, Influence of manufacturing conditions on the bioavailability of magnesium in calcined magnesites measured in vivo and in vitro, J. Agric. Sci. 127 (3) (1996) 377–385.
[3] J.F. He, X. Zhang, Q. Bai, S.B. Huang, H. Chen, C.J. Guo, L.T. Zhu, B. Yang, Surface modification to enhance the decarbonization performance of coal-series kaolin by triboelectric separation, Appl. Clay Sci. 235 (2023) 106857.
[4] X.F. Gong, J. Yao, B. Yang, W.Z. Yin, J. Guo, N.B. Song, Y.L. Wang, H.R. Sun, Activation–inhibition mechanism of diammonium hydrogen phosphate in flotation separation of brucite and calcite, J. Environ. Chem. Eng. 11 (3) (2023) 110184.
[5] B. Yang, L.T. Zhu, J.F. He, W.Z. Yin, J. Yao, A feasible strategy for depressant-free flotation separation of siderite from magnesiohornblende using a highly selective collector, J. Mol. Liq. 394 (2024) 123689.
[6] X.F. Gong, J. Yao, B. Yang, W.Z. Yin, Y.L. Wang, Y.F. Fu, Adsorption mechanism of green efficient chelating poly-L-aspartic acid in flotation separation of brucite and dolomite, Adv. Powder Technol. 34 (11) (2023) 104207.
[7] X.F. Gong, J. Yao, B. Yang, W.Z. Yin, Y.L. Wang, Y.F. Fu, Selective adsorption of the activator diammonium hydrogen phosphate in the reverse flotation separation of brucite and dolomite, Powder Technol. 429 (2023) 118923.
[8] H.R. Sun, B. Yang, Z.L. Zhu, W.Z. Yin, Q.Y. Sheng, Y. Hou, J. Yao, New insights into selective-depression mechanism of novel depressant EDTMPS on magnesite and quartz surfaces: adsorption mechanism, DFT calculations, and adsorption model, Miner. Eng. 160 (2021) 106660.
[9] W.Z. Yin, H.R. Sun, J. Hong, S.H. Cao, B. Yang, C. Won, M. Song, Effect of Ca selective chelator BAPTA as depressant on flotation separation of magnesite from dolomite, Miner. Eng. 144 (2019) 106050.
[10] X.F. Gong, J. Yao, B. Yang, J. Guo, H.R. Sun, W.Z. Yin, Study on the inhibition mechanism of guar gum in the flotation separation of brucite and dolomite in the presence of SDS, J. Mol. Liq. 380 (2023) 121721.
[11] Q.C. Feng, W.H. Yang, S.M. Wen, H. Wang, W.J. Zhao, G. Han, Flotation of copper oxide minerals: a review, Int. J. Min. Sci. Technol. 32 (6) (2022) 1351–1364.
[12] Z.L. Zhu, Y.F. Fu, W.Z. Yin, H.R. Sun, K.Q. Chen, Y. Tang, B. Yang, Role of surface roughness in the magnesite flotation and its mechanism, Particuology 62 (2022) 63–70.
[13] W.X. Zhong, W.Z. Yin, Y.L. Wang, J. Yao, Selective flotation of magnesite from dolomite using α-chloro-oleate acid as collector, Powder Technol. 373 (2020) 147–151.
[14] Z.L. Zhu, W.Z. Yin, D.H. Wang, H.R. Sun, K.Q. Chen, B. Yang, The role of surface roughness in the wettability and floatability of quartz particles, Appl. Surf. Sci. 527 (2020) 146799.
[15] Ö. Bıçak, Z. Ekmekçi, M. Can, Y. Öztürk, The effect of water chemistry on froth stability and surface chemistry of the flotation of a Cu–Zn sulfide ore, Int. J. Miner. Process 102-103 (2012) 32–37.
[16] L.P. Luo, L.H. Xu, X.Z. Shi, J.P. Meng, R.H. Liu, Microscale insights into the influence of grinding media on spodumene micro-flotation using mixed anionic/cationic collectors, Int. J. Min. Sci. Technol. 32 (1) (2022) 171–179.
[17] P.E. Sarquís, J.M. Menéndez-Aguado, M.M. Mahamud, R. Dzioba, Tannins: the organic depressants alternative in selective flotation of sulfides, J. Clean. Prod. 84 (2014) 723–726.
[18] L.M. Yang, Z. Gao, T. Liu, M.T. Huang, G.Z. Liu, Y.F. Feng, P.H. Shao, X.B. Luo, Direct electrochemical leaching method for high-purity lithium recovery from spent lithium batteries, Environ. Sci. Technol. 57 (11) (2023) 4591–4597.
[19] L.O. Filippov, L.A. Silva, A.M. Pereira, L.C. Bastos, J.C.G. Correia, K. Silva, A. Piçarra, Y. Foucaud, Molecular models of hematite, goethite, kaolinite, and quartz: surface terminations, ionic interactions, nano topography, and water coordination, Colloids Surf. A Physicochem. Eng. Aspects 650 (2022) 129585.
[20] G.L. Zhu, Y.H. Zhao, X.Y. Zheng, Y.H. Wang, H.T. Zheng, D.F. Lu, Surface features and flotation behaviors of spodumene as influenced by acid and alkali treatments, Appl. Surf. Sci. 507 (2020) 145058.
[21] N.N. Zhang, M. Ejtemaei, A.V. Nguyen, C.C. Zhou, XPS analysis of the surface chemistry of sulfuric acid-treated kaolinite and diaspore minerals with flotation reagents, Miner. Eng. 136 (2019) 1–7.
[22] P.S. Parapari, M. Irannajad, A. Mehdilo, Modification of ilmenite surface properties by superficial dissolution method, Miner. Eng. 92 (2016) 160–167.
[23] P. Semsari Parapari, M. Irannajad, A. Mehdilo, Effect of acid surface dissolution pretreatment on the selective flotation of ilmenite from olivine and pyroxene, Int. J. Miner. Process. 167 (2017) 49–60.
[24] B. Feng, Y.P. Lu, Q.M. Feng, M.Y. Zhang, Y.L. Gu, Talc–serpentine interactions and implications for talc depression, Miner. Eng. 32 (2012) 68–73.
[25] X.F. Gong, J. Yao, B. Yang, Y.F. Fu, Y.L. Wang, W.Z. Yin, Selective flotation of brucite from calcite using HEDP-4Na as an inhibitor in a SDS system, J. Ind. Eng. Chem. 125 (2023) 390–401.
[26] B. Yang, D.H. Wang, S.H. Cao, W.Z. Yin, J.W. Xue, Z.L. Zhu, Y.F. Fu, J. Yao, Selective adsorption of a high-performance depressant onto dolomite causing effective flotation separation of magnesite from dolomite, J. Colloid Interface Sci. 578 (2020) 290–303.
[27] X.F. Gong, J. Yao, B. Yang, W.Z. Yin, J. Guo, N.B. Song, Y.L. Wang, H.R. Sun, Y.F. Fu, Selective activation of new regulator SMP in reverse flotation separation of brucite and calcite, Colloids Surf. A Physicochem. Eng. Aspects 675 (2023) 132049.
[28] A. Hassanzadeh, D. Huu Hoang, M. Brockmann, Assessment of flotation kinetics modeling using information criteria; case studies of elevated-pyritic copper sulfide and high-grade carbonaceous sedimentary apatite ores, J. Dispers. Sci. Technol. 41 (7) (2020) 1083–1094.
[29] H.J. Zhang, J.T. Liu, Y.J. Cao, Y.T. Wang, Effects of particle size on lignite reverse flotation kinetics in the presence of sodium chloride, Powder Technol. 246 (2013) 658–663.
[30] R.D. Stanojlovi, J.M. Sokolovi, A study of the optimal model of the flotation kinetics of copper slag from copper mine BOR, Arch. Min. Sci. 59 (3) (2014) 821–834.
[31] X.M. Yuan, B.I. Palsson, K.S.E. Forssberg, Statistical interpretation of flotation kinetics for a complex sulphide ore, Miner. Eng. 9 (4) (1996) 429–442.
[32] S.H. Cao, W.Z. Yin, B. Yang, Z.L. Zhu, H.R. Sun, Q.Y. Sheng, K.Q. Chen, Insights into the influence of temperature on the adsorption behavior of sodium oleate and its response to flotation of quartz, Int. J. Min. Sci. Technol. 32 (2) (2022) 399–409.
[33] C.J. Fang, S.C. Yu, X.Y. Wei, H. Peng, L.M. Ou, G.F. Zhang, J. Wang, The cation effect on adsorption of surfactant in the froth flotation of low-grade diasporic bauxite, Miner. Eng. 144 (2019) 106051.
[34] M.Y. Li, C. Yang, Z.Y. Wu, X.P. Gao, X. Tong, X.K. Yu, H.M. Long, Selective depression action of taurine in flotation separation of specularite and chlorite, Int. J. Min. Sci. Technol. 32 (3) (2022) 637–644.
[35] Z.L. Zhu, D.H. Wang, B. Yang, W.Z. Yin, M.S. Ardakani, J. Yao, J.W. Drelich, Effect of nano-sized roughness on the flotation of magnesite particles and particle-bubble interactions, Miner. Eng. 151 (2020) 106340.
[36] X.F. Gong, J. Yao, B. Yang, Z.L. Zhu, J. Guo, W.Z. Yin, Y.F. Fu, Y.L. Wang, An environment-friendly and highly effective inhibitor for flotation separation of brucite and dolomite in SDS system, Sep. Sci. Technol. 58 (10) (2023) 1784–1794.
[37] N.N. Zhang, T. Pang, R. Han, Z.L. Zhu, Z. Li, Insight into anionic and cationic flotation discrepancy of quartz with altered surface roughness by acid etching, J. Mol. Liq. 381 (2023) 121816.
[38] Z.L. Zhu, Z. Li, W.Z. Yin, B. Yang, N.N. Zhang, J.Z. Qu, S.J. Chen, J. Chang, Y.X. Yu, L.J. Liu, Effect of surface roughness on the flotation separation of hematite from fine quartz, J. Ind. Eng. Chem. 109 (2022) 431–441.
[39] B. Vaziri Hassas, H. Caliskan, O. Guven, F. Karakas, M. Cinar, M.S. Celik, Effect of roughness and shape factor on flotation characteristics of glass beads, Colloids Surf. A Physicochem. Eng. Aspects 492 (2016) 88–99.